リポソーム、β-gal を除去した。この細胞を培地に再懸濁し、スライドチャンバーガラスに播種し、4 時間培養した。その後、X-gal 染色を行い、顕微鏡による観察を行った。

13. LF2000 およびバブルリポソームと超音波の併用によるβ-gal 導入細胞の観察

スライドチャンバーガラスに 4T1-Luc 細胞を 1.5×10^5 cells/well 播種し、CO_2 インキュベーターで一日培養した。その後、PBS で細胞を洗浄し、β-gal (1 μg) と LF2000 (2 μL) の複合体を添加し、4 時間培養した。その後、バブルリポソーム (総脂質量 : 60 μg) を加え Opti-MEM で総量を 500 μL にし、速やかに超音波 (Frequency : 2 MHz, Duty : 50%, Burst Rate : 2 Hz, Intensity : 1.0, 2.0, 2.5 W/cm^2, Time : 10 sec. 1, 3 回) 照射した。細胞を洗浄し余剰のバブルリポソームを除去し、培地を加え 1 時間培養した。その後、X-gal 染色を行い、顕微鏡による観察を行った。

C. 研究結果

結果は D 項にまとめて記載。

D. 考 察

1. バブルリポソームと超音波照射の併用により生じるキャビテーションにより siRNA が分解されてしまっては、本方法の siRNA 導入への応用が困難になる。そこで、バブルリポソームと超音波照射の併用による siRNA への影響を検討した (Fig.1)。電気泳動の結果、無処理の siRNA のバンドと比較して超音波照射のみ、超音波とバブルリポソームを併用した siRNA のバンドの顕著な消失は認められなかった。このことより、バブルリポソームと超音波の併用による siRNA の分解はないものと考えられた。

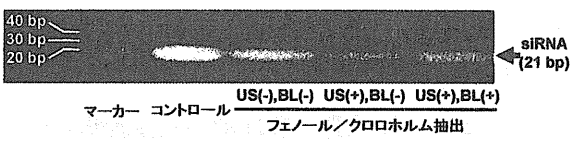

Fig.1 キャビテーションによる siRNA への影響評価

siRNA (150 nM) にバブルリポソーム (60 μg) を加え、速やかに超音波 (Frequency : 2 MHz, Duty : 50 %, Burst Rate : 2 Hz, Intensity : 2.5 W / cm^2, Time : 10 sec.) 照射した。超音波照射後、フェノール/クロロホルム抽出した。siRNA をエタノール沈殿にて濃縮後、ポリアクリルアミド電気泳動し、siRNA への影響を評価した。US : 超音波照射, BL : バブルリポソーム

2. バブルリポソームと超音波照射の併用により siRNA を細胞内に導入可能であることを確認するため、本導入法によるプラスミド DNA と siRNA の共導入による遺伝子発現抑制効果を検討した。なお今回の検討では、ルシフェラーゼ (GL2 配列) 発現プラスミド DNA (pGL2) とルシフェラーゼ (GL2 配列) の発現を抑制する siRNA (GL2 siRNA)、EGFP (enhanced green fluorescent protein) 発現

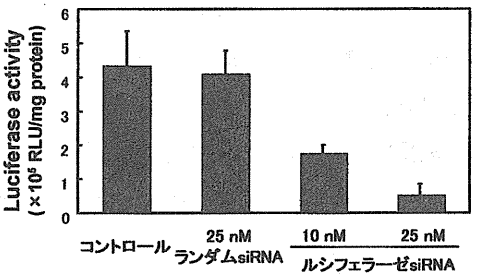

Fig.2 ルシフェラーゼ遺伝子とルシフェラーゼ siRNA 共導入

COS-7 細胞 (1×10^5 cells / tube) に pGL2 (5 μg) と GL2 siRNA (5 pmol, 12.5 pmol)、およびバブルリポソーム (60 μg) を添加し、超音波 (Frequency : 2 MHz, Duty : 50 %, Burst Rate : 2.0 Hz, Intensity : 2.5 W / cm^2, Time : 10 sec.) 照射した。細胞を 2 回洗浄し、37℃、5 %CO_2 で 24 時間培養した。培養後、ルシフェラーゼ活性の測定を行った。なお、ルシフェラーゼ活性は RLU/ mg protein で示した。

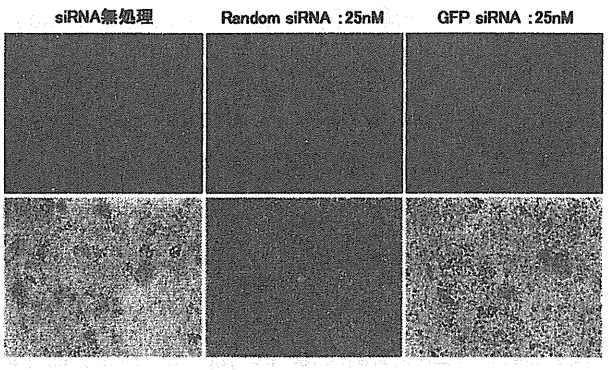

Fig. 3 EGFP 遺伝子と EGFP siRNA 共導入

COS-7 細胞 (1×10^5 cells/tube) に pEGFP-C1 (5 μg) と EGFP siRNA (12.5 pmol)、およびバブルリポソーム (60 μg) を添加し、超音波 (Frequency : 2 MHz, Duty : 50 %, Burst Rate : 2 Hz, Intensity : 2.5 W/cm^2, Time : 10 sec.) 照射した。細胞を 2 回洗浄し、37℃、5 %CO_2 で 24 時間培養した。培養後、蛍光顕微鏡により EGFP の発現を観察した。上段 : EGFP, 下段 : 位相差

プラスミド DNA（pEGFP-C1）と EGFP の発現を抑制する siRNA（EGFP siRNA）を用いて検討した(Fig.,2, 3)。また、ネガティブコントロールとしてランダム配列の siRNA（ランダム siRNA）を用いた。pGL2 および GL2 siRNA の共導入を行った結果、pGL2 のみを導入したコントロール群と比較して、ルシフェラーゼ siRNA 作用群において siRNA 濃度依存的な発現抑制が観察された。そして、この発現抑制率は GL2 siRNA 25 nM 作用群で約 90% に達した。また、この抑制はランダム siRNA 作用群ではほとんど認められず、今回の結果が配列特異的なルシフェラーゼ発現抑制であることが確認された（Fig.2)。さらに pEGFP-C1 および EGFP siRNA の共導入においても、siRNA 無処理のコントロール群と比較してランダム siRNA 作用群ではほとんど EGFP 発現抑制が認められなかった。一方、EGFP siRNA 作用群では顕著な EGFP 発現抑制が観察された(Fig.3)。また、今回の検討条件におけるキャビテーション誘導による細胞への傷害性を評価した結果、顕著な細胞生存率の低下は確認されなかった（Fig.4)。

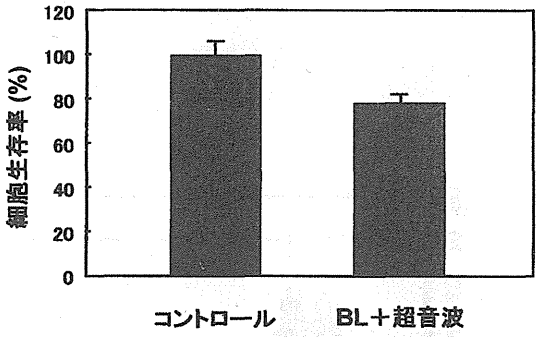

Fig.4 キャビテーションによる細胞傷害性

COS-7 細胞（1×10^5 cells/tube）にバブルリポソーム（60 μg）を加え、超音波照射した。超音波照射条件は Frequency：2 MHz, Duty：50 %, Burst Rate：2.0 Hz, Intensity：2.5 W/cm^2, Time：10 sec. で検討した。細胞を洗浄し、48 時間培養後、MTT-Assay により細胞傷害性を評価した。BL：バブルリポソーム

3. バブルリポソームを用いて導入した siRNA の恒常発現たん白質に対する発現抑制に関して検討した。なお、今回の検討では Colon-26 細胞にルシフェラーゼ（GL3 配列）発現プラスミド DNA（pCMV-Luc）を導入し、ルシフェラーゼを恒常発現させたルシフェラーゼ発現 Colon-26 細胞とルシフェラーゼ siRNA（GL3 siRNA）を用いて検討した。また、ネガティブコントロールとしてルシフェラーゼと相補性のない EGFP siRNA を用いた検討も行った(Fig.5)。その結果、siRNA 無処理のコントロール群と比較して EGFP siRNA 作用群ではほとんどルシフェラーゼ発現抑制が認められなかった。一方、ルシフェラーゼ siRNA 導入群では約 45% のルシフェラーゼ発現抑制が観察された。このことより、本方法を用いた siRNA 導入は、恒常発現しているたん白質の発現抑制も可能であることが確認された。

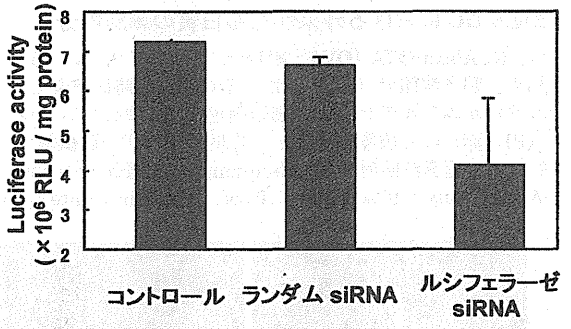

Fig.5 ルシフェラーゼ恒常発現細胞へのルシフェラーゼ siRNA の導入

ルシフェラーゼ恒常発現 Colon-26 細胞（1×10^5 cells/tube）とバブルリポソーム(60 μg)、および GL3 siRNA(100 pmol)を添加し、超音波（Frequency：2 MHz, Duty：10%, Burst Rate：2 Hz, Intensity：2.5 W/cm^2, Time：10 sec.）照射した。細胞を 2 回洗浄し、37℃、5 %CO_2 で 24 時間培養した。培養後、ルシフェラーゼ活性の測定を行った。なお、ルシフェラーゼ活性は RLU/ mg protein で示した。

4. バブルリポソームと超音波照射による細胞内へのたん白質デリバリー効率を評価するため、モデルたん白質として Alexa488 で蛍光ラベルしたニワトリ卵白アルブミン（Alexa-OVA）を用い検討した(Fig.6)。DC に Alexa-OVA を添加した群、Alexa-OVA とバブルリポソームを添加した群、Alexa-OVA を添加し超音波照射した群では細胞内にドット状の Alexa-OVA が観察された。これはエンドサイトーシスにより取り込まれた Alexa-OVA と考えられる。一方、Alexa-OVA とバブルリポソームを添加し、超音波照射した群ではドット状の Alexa-OVA に加え、細胞質内に広く分布しているのが認められた。これはエンドサイトーシス経路で取り込まれたドット状の Alexa-OVA とエンドサイトーシス非依存的に送達された Alexa-OVA が同時に観察されたと考えられる。

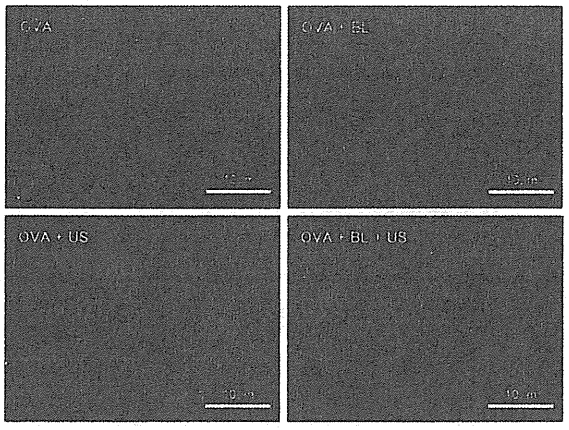

Fig.6 DC における外来性たん白質の細胞内分布

DC に Alexa-OVA (OVA : 緑)とバブルリポソーム (BL) を加え、超音波照射 (US) した。その後、1 時間培養し、3% パラホルムアルデヒドにて細胞固定し、ヨウ化プロピジウム (PI : 赤) にて核染色を行い、共焦点レーザー顕微鏡にて観察した。超音波照射条件 (Frequency : 2 MHz, Intensity : 2 W/cm², Duty : 10%, Time : 10 sec. 3 回, Burst Rate : 2 Hz)

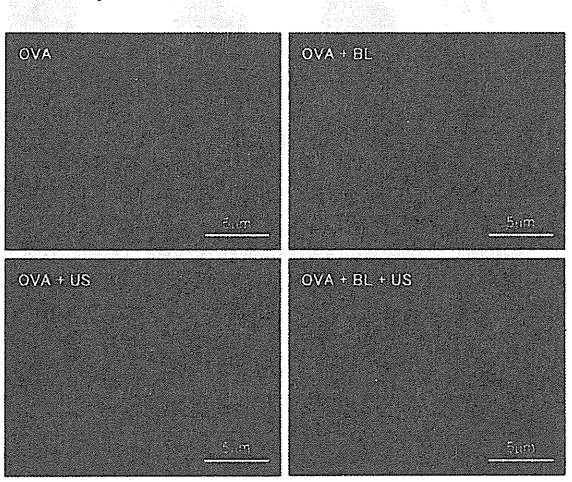

Fig.7 エンドサイトーシス阻害下における外来性たん白質の送達

DC に 10 mM アジ化ナトリウムを添加し、4℃下で Alexa-OVA (OVA : 緑) とバブルリポソーム (BL) を加え、超音波照射 (US) した。その後、3% パラホルムアルデヒドにて細胞固定し、ヨウ化プロピジウム (PI : 赤) にて核染色を行い、共焦点レーザー顕微鏡にて観察した。超音波照射条件 (Frequency : 2 MHz, Intensity : 2 W/cm², Duty : 10%, Time : 10 sec. 3 回, Burst Rate : 2Hz)

次に、バブルリポソームと超音波による DC への Alexa-OVA の取り込みをエンドサイトーシス阻害下で観察した (Fig.7)。その結果、DC に Alexa-OVA を添加した群、Alexa-OVA とバブルリポソームを添加した群、Alexa-OVA を添加し超音波照射した群では Alexa-OVA による蛍光は観察されなかった。一方、Alexa-OVA とバブルリポソームを添加し、超音波照射した群ではエンドサイトーシス阻害下にもかかわらず、細胞質内でバブルリポソームと超音波照射の併用法はエンドサイトーシスを介さず、外来性たん白質を細胞質に直接導入可能な方法であることが示唆された。さらに、本方法によるエンドサイトーシス非依存的な外来性たん白質の導入効率について検討した。上述と同様の方法でエンドサイトーシスを阻害し、Alexa-OVA とバブルリポソームを加え、超音波照射した。その後、細胞を洗浄し、外来性たん白質の導入率をフローサイトメトリーにて解析した (Fig.8)。その結果、DC に Alexa-OVA を加えた群、Alexa-OVA とバブルリポソームを加えた群、Alexa-OVA を加え超音波照射した群の導入効率はそれぞれ 4.4%、5.4%、6.9%と低い値であった。一方、Alexa-OVA とバブルリポソームを加え超音波照射した群の導入効率は 30.6% と高い値を示した。このようにバブルリポソームと超音波の併用により、外来性のたん白質が細胞質内に導入されること、またその導入効率が約 30% であることが明らかとなった。このようにバブルリポソームと超音波の併用法が、分子量4万5千の OVA を、エンドサイトーシス経路を介さず細胞質内に導入可能であることが明らかとなった。

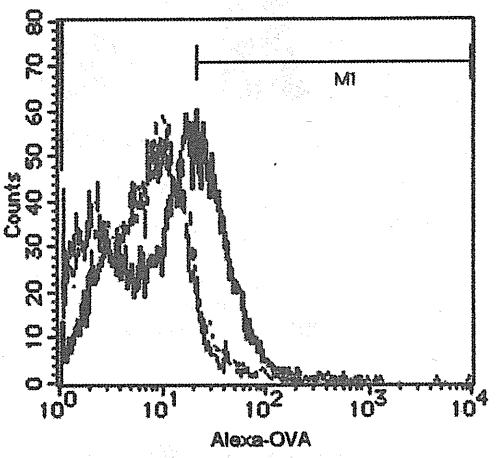

Fig.8 エンドサイトーシス阻害下における外来性たん白質の送達効率

DC に 10 mM アジ化ナトリウムを添加し、4℃ 下で Alexa-OVA とバブルリポソーム (BL) を加え、超音波照射 (US) した。その後、フローサイトメトリーにより送達効率を解析した。なお、本実験では Alexa-OVA を加えない群を control とした。超音波照射条件 (Frequency : 2 MHz, Intensity : 2 W/cm², Duty : 10%, Time : 10 sec. 3 回, Burst Rate : 2 Hz)

5. バブルリポソームと超音波照射の併用による外来性物質の細胞内デリバリーにおける特性を評価するため、分子量の異なる FITC-デキストランを用いて検討をおこなった。その結果、いずれの分子量の FITC-デキストランであっても細胞内にデリバリーできることが明らかとなった。これは、本デリバリー法が細胞膜に一過性の小孔をあけて外来性物質をデリバリーする方法であるため、様々な分子量の分子も細胞内に導入できたものと考えられた。次に、デリバリー効率におよぼす分子量の影響を検討した。その結果、FITC－デキストランの分子量が大きくなるにつれて、徐々に細胞内へのデリバリー効率が低下することが明らかとなった。これは、バブルリポソームと超音波の併用により生じる細胞膜上の小孔の大きさは一定であるため、分子サイズの大きな分子が透過しにくかったためと考えられた。いずれにしても、本方法では様々な分子を細胞内に導入できる方法であることが示された。

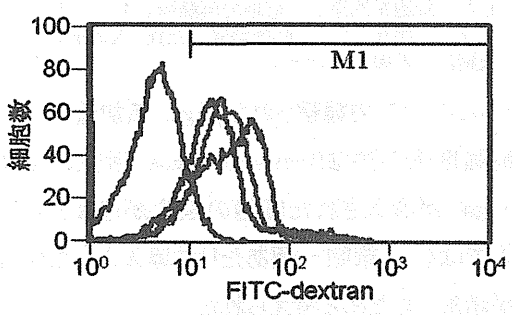

	平均蛍光強度	% of M1 gated
Non-treat	5.7	6.6
Mw: 4,000	24.5	86.0
Mw: 20,000	22.4	87.3
Mw: 70,000	16.5	77.4

Fig.9 FITC-デキストランの送達効率
DC に 10 mM アジ化ナトリウムを添加し、4℃ 下で FITC-デキストランとバブルリポソーム (BL) を加え、超音波照射 (US) した。その後、フローサイトメトリーにより送達効率を解析した。なお、本実験では FITC-デキストランを加えない群を control とした。超音波照射条件 (Frequency : 2 MHz, Intensity : 2 W/cm², Duty : 10%, Time : 10 sec. 3 回, Burst Rate : 2 Hz)

6. バブルリポソームと超音波照射の併用による細胞内へのβ-gal 導入効率を評価するにあたり、ポジティブコントロールとして既存の遺伝子導入試薬である LF2000 によるβ-gal の細胞内への導入効率を検討した(Fig.10)。その結果、β-gal/LF2000 複合体の添加量の増加に伴い、β-galactosidase 活性の上昇が認められた。このことから、LF2000 によりβ-gal が細胞内に導入されていることが明らかとなった。

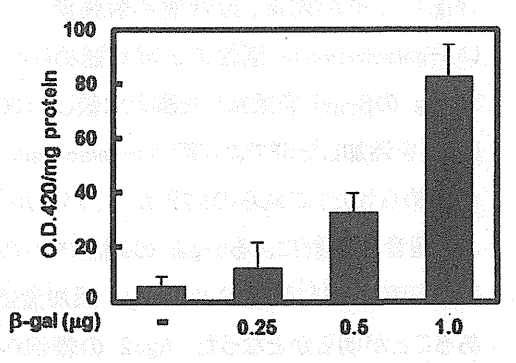

Fig.10 LF2000 によるβ-gal 導入効率の検討
β-gal (0.25, 0.5, 1.0 μg) と LF2000 (0.5, 1.0, 2.0 μL) を 4T1-Luc 細胞 (3×10^4 cells/well) に添加し、4 時間培養した。その後、β-galactosidase 活性を測定した。

7. siRNA による効率的な遺伝子発現抑制効果を得るためには、多くの細胞に siRNA と Ago2 を導入することが必要となる。そこで、バブルリポソームと超音波照射の併用によるβ-gal 導入細胞を評価するにあたり、ポジティブコントロールとして既存の遺伝子導入試薬である LF2000 によるβ-gal 導入細胞の観察を行った(Fig.11)。その結果、β-gal/LF2000 複合体添加群において、X-gal 染色により青く染まった細胞が観察されたが、その細胞は一部であった。このことから、LF2000 は一部の細胞にβ-gal を導入していることが明らかとなった。

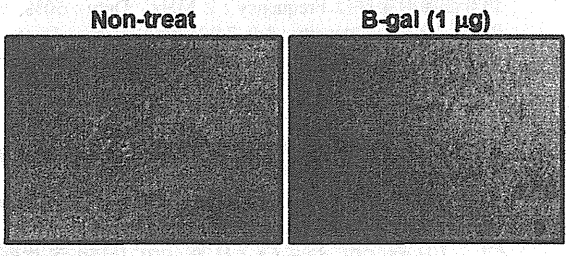

Fig.11 LF2000 によるβ-gal 導入細胞の観察
β-gal (1.0 μg) と LF2000 (2.0 μL) を 4T1-Luc 細胞 (5×10^4 cells/well) に添加し、4 時間培養した。その後、X-gal 染色を行い顕微鏡による観察を行った。

8. バブルリポソームと超音波照射の併用による細胞内へのβ-gal 導入効率について検討した。β-gal 添

加量は 50 μg もしくは 100 μg とした。これまでの本研究室での研究において、超音波照射強度は遺伝子やたん白質の細胞内への導入効率に影響を与える重要なパラメーターであることを確認している。そのため、1.0 W/cm^2 および 2.0 W/cm^2 の超音波照射強度におけるβ-gal 導入効率を検討した(Fig.12)。その結果、超音波照射強度の増大に伴いβ-galactosidase 活性の上昇が認められた。また、50 μg のβ-gal を添加した群と比較し、100 μg のβ-gal を添加した群でより高いβ-galacotsidase 活性が認められた。これらの結果から、バブルリポソームと超音波照射によるβ-gal の細胞内への導入効率は超音波照射強度およびβ-gal 添加量依存的であることが明らかとなった。Ago2 の細胞内への導入においても、同様に超音波照射強度およびたん白質添加量が重要なパラメーターとなると考えられる。

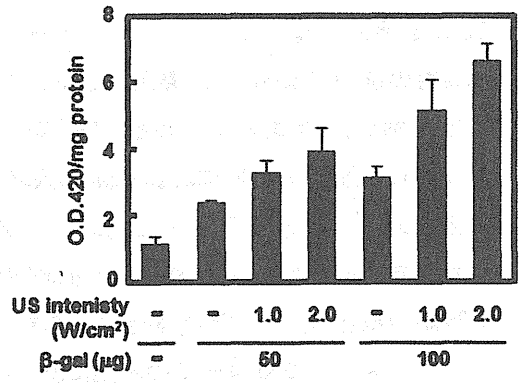

Fig.12 バブルリポソームと超音波によるβ-gal 導入効率の検討
4T1-Luc 細胞 (2×10^6 cells/tube) にβ-gal (50, 100 μg) およびバブルリポソーム (60 μg) を加え、超音波照射した。超音波照射条件は Frequency : 2 MHz、Duty : 50%、Burst Rate : 2.0 Hz、Intensity : 1.0, 2.0 W/cm^2、Time : 10 sec. 3 回で検討した。細胞を洗浄し、4 時間培養後、β-galactosidase 活性を測定した。

9. バブルリポソームと超音波照射によるβ-gal 導入細胞を検討した。β-gal 添加量を 50 μg もしくは 100 μg とし、1.0 W/cm^2 および 2.0 W/cm^2 の超音波照射強度におけるβ-gal 導入細胞を評価した(Fig.13)。その結果、X-gal 染色により青く染まっている細胞が一部観察された。しかしながら、β-gal 添加量、超音波照射強度の増加に伴う、X-gal により染色された細胞の割合の増大は認められなかった。このことから、Fig.12 で観察されたβ-gal 添加量、超音波照射強度依存的なβ-galactosidase 活性の上昇は、β-gal が導入された細胞の割合が増えたことが原因ではなく、細胞一個あたりに導入されたβ-gal 量が増加したためと考えられた。

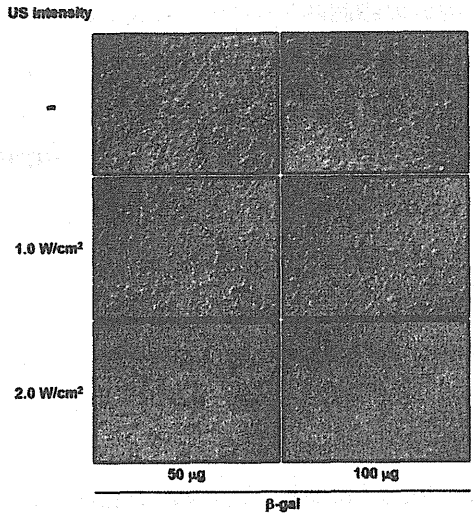

Fig.13 バブルリポソームと超音波によるβ-gal 導入細胞の観察
4T1-Luc 細胞 (2.5×10^5 cells/tube) にβ-gal (50, 100 μg) およびバブルリポソーム (60 μg) を加え、超音波照射した。超音波照射条件は Frequency : 2 MHz、Duty : 50%、Burst Rate : 2.0 Hz、Intensity : 1.0, 2.0 W/cm^2、Time : 10 sec. 3 回で検討した。細胞を洗浄し、培地で再懸濁しスライドチャンバーガラスに播種した。4 時間培養した後、X-gal 染色を行い顕微鏡による観察を行った。

10. siRNA と Ago2 による高い遺伝子発現抑制効果を得るためには、siRNA と Ago2 を細胞質へ導入することが必要となる。一般的にエンドサイトーシス経路を介した核酸、たん白質デリバリーでは、エンドソームからリソソームに輸送され分解を受けるために、細胞質への移行量が減少してしまう。これまでに、バブルリポソームと超音波照射の併用は、遺伝子キャリアーのエンドソームエスケープを促進し、遺伝子発現効率を上昇させることを明らかとしている。そこで、LF2000 によりβ-gal を細胞内へ取り込ませた後に、バブルリポソームと超音波照射を併用した際のβ-gal 導入細胞について観察した(Fig.14)。その結果、LF2000 によりβ-gal を導入した群と比較し、バブルリポソームと超音波照射を併用した群での、X-gal 染色により青く染まった細胞の割合が若干増加した。このことから、β-gal を細胞内に取り込ませた後に、バブルリポソームと超音波

を併用することで、リソソームによる分解を回避し、細胞質へ効率的にデリバリーできることが示唆された。

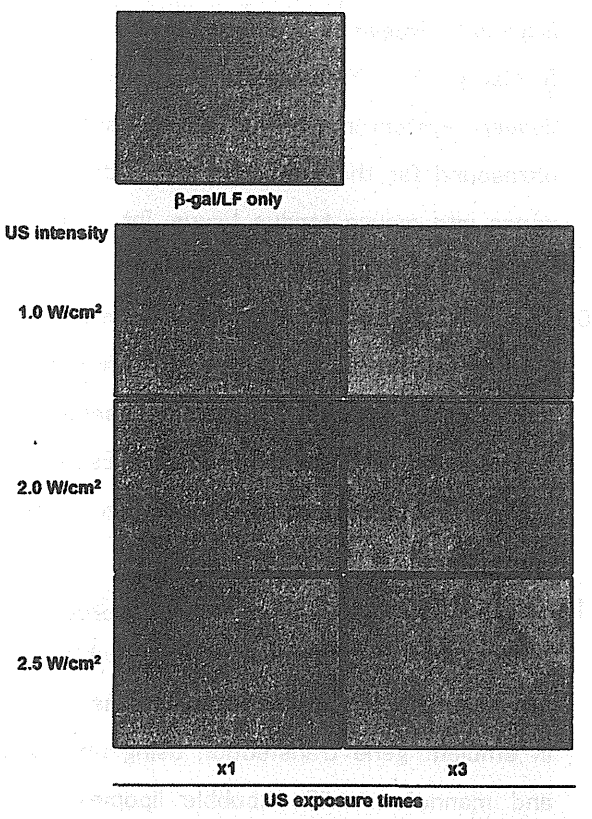

Fig.14 LF2000 およびバブルリポソームと超音波の併用によるβ-gal 導入細胞の観察
4T1-Luc 細胞 (1.5×10^5 cells/well) にβ-gal (1 μg) と LF2000 (1 μL) の複合体を添加し、4 時間培養した。その後、バブルリポソーム (60 μg) を加え、超音波照射した。超音波照射条件は Frequency : 2 MHz、Duty : 50%、Burst Rate : 2.0 Hz、Intensity : 1.0, 2.0, 2.5 W/cm²、Time : 10 sec. 3 回で検討した。細胞を洗浄し、培地で再懸濁しスライドチャンバーガラスに播種した。1 時間培養した後、X-gal 染色を行い顕微鏡による観察を行った。

E. 結論

バブルリポソームと超音波照射の併用による siRNA および Ago2 デリバリーの同時デリバリー方法の確立に向けて、本導入方法の特性を評価した。まず、siRNA のデリバリーについて検討したところ、本デリバリー法により細胞内に siRNA が導入可能であること、またその結果配列特異的な遺伝子発現抑制効果が認められた。Ago2 導入については、Ago2 のたん白質の大量精製の系を研究代表者が検討しているため、本研究ではモデルたん白質を利用して導入特性を評価した。まず、本導入方法の導入効率におよぼす分子量特性の評価を目的に FITC-デキストランの導入効率を評価した。その結果、分子量が大きくなるにつれてデリバリー効率が徐々に低下する傾向が認められた。しかし、本デリバリー法で様々な分子を導入できる可能性が見出された。そこで、次にモデルたん白質を利用した導入特性を評価した。その結果、エンドサイトーシス阻害下でも細胞内にたん白質が導入されることが明らかとなった。このことから、バブルリポソームと超音波照射の併用では、エンドサイトーシス経路を介さずに外来性物質を細胞質内に導入できる

次に Ago2 (106 kDa) と分子量の近いβ-ガラクトシダーゼ (β-gal) (116 kDa) を用い、細胞内へのデリバリー効率について評価した。その結果、バブルリポソームと超音波により細胞内にβ-gal の酵素活性を維持したまま導入可能であることが明らかとなった。このことから、Ago2 に対してもその活性を維持したまま細胞質内に導入可能になるのではないかと期待される。しかし、LF2000 と比較し、バブルリポソームと超音波によるβ-gal 導入効率、β-gal 導入細胞の割合は低く、超音波導入条件の更なる最適化が必要と考えられた。この問題を改善するために、バブルリポソームと超音波照射によるエンドサイトーシス脱出による β-gal 導入を試みた。LF2000 とβ-gal 複合体を細胞に取り込ませた後、バブルリポソームと超音波照射を適用すると LF2000 単独導入よりその効率は改善された。このことから、バブルリポソームと超音波照射により、β-gal のエンドソームエスケープを促進できる可能性が示された。

今回の検討では、実際に Ago2 たん白質を用いた検討を行うことはできなかった。しかし、今回の検討で siRNA やモデルたん白質の細胞質内導入が可能であることを見出した。それゆえ、バブルリポソームと超音波照射の併用が、siRNA と Ago2 たん白質の同時デリバリーにも適用可能であると考えられる。

F. 健康危険情報

なし

G-1 論文発表

1. Negishi Y, Hamano N, Shiono H, Akiyama S, Endo-Takahashi Y, Suzuki R, Maruyama K, Aramaki Y.: The development of an ultrasound-mediated nucleic acid delivery

system for treating muscular dystrophies. Yakugaku Zasshi, 132: 1383-1388 (2012)

2. Negishi Y, Endo-Takahashi Y, Matsuki Y, Kato Y, Takagi N, Suzuki R, Maruyama K, Aramaki Y.: Systemic delivery systems of angiogenic gene by novel bubble liposomes containing cationic lipid and ultrasound exposure. Mol. Pharm., 9:1834-1840 (2012)
3. Sonoda S, Tachibana K, Yamashita T, Shirasawa M, Terasaki H, Uchino E, Suzuki R, Maruyama K, Sakamoto T.: Selective gene transfer to the retina using intravitreal ultrasound irradiation. J. Ophthalmol., 2012: 412752 (2012)
4. Omata D, Negishi Y, Yamamura S, Hagiwara S, Endo-Takahashi Y, Suzuki R, Maruyama K, Nomizu M, Aramaki Y.: Involvement of Ca2+ and ATP in enhanced gene delivery by bubble liposomes and ultrasound exposure. Mol. Pharm., 9: 1017-1023 (2012)
5. Omata D, Negishi Y, Hagiwara S, Yamamura S, Endo-Takahashi Y, Suzuki R, Maruyama K, Aramaki Y.: Enhanced gene delivery using Bubble liposomes and ultrasound for folate-PEG liposomes. J. Drug Target., 20: 355-363 (2012)
6. Un K, Kawakami S, Yoshida M, Higuchi Y, Suzuki R, Maruyama K, Yamashita F, Hashida M.: Efficient suppression of murine intracellular adhesion molecule-1 using ultrasound-responsive and mannose-modified lipoplexes inhibits acute hepatic inflammation. Hepatology, 56: 259-269 (2012)
7. Oda Y, Suzuki R, Otake S, Nishiie N, Hirata K, Koshima R, Nomura T, Utoguchi N, Kudo N, Tachibana K, Maruyama k.: Prophylactic immunization with Bubble liposomes and ultrasound-treated dendritic cells provided a four-fold decrease in the frequency of melanoma lung metastasis. J. Control. Release, 160: 362-366 (2012)
8. Endo-Takahashi Y, Negishi Y, Kato Y, Suzuki R, Maruyama K, Aramaki Y.: Efficient siRNA delivery using novel siRNA-loaded Bubble liposomes and ultrasound. Int. J. Pharm. 422: 504-509 (2012)
9. Sugano M, Negishi Y, Endo-Takahashi Y, Suzuki R, Maruyama K, Yamamoto M, Aramaki Y.: Gene delivery system involving Bubble liposomes and ultrasound for the efficient in vivo delivery of genes into mouse tongue tissue. Int. J. Pharm. 422: 332-337 (2012)
10. Omata D, Negishi Y, Hagiwara S, Yamamura S, Endo-Takahashi Y, Suzuki R, Maruyama K, Nomizu M, Aramaki Y.: Bubble Liposomes and Ultrasound Promoted Endosomal Escape of TAT-PEG Liposomes as Gene Delivery Carriers. Mol Pharm., 8: 2416-2423 (2011)
11. Un K, Kawakami S, Higuchi Y, Suzuki R, Maruyama K, Yamashita F, Hashida M.: Involvement of activated transcriptional process in efficient gene transfection using unmodified and mannose-modified bubble lipoplexes with ultrasound exposure. J Control Release 156: 355-363 (2011)
12. Shiraishi K, Endoh R, Furuhata H, Nishihara M, Suzuki R, Maruyama K, Oda Y, Jo J, Tabata Y, Yamamoto J, Yokoyama M.: A facile preparation method of a PFC-containing nano-sized emulsion for theranostics of solid tumors. Int J Pharm, 421: 379-387 (2011)
13. Un K, Kawakami S, Suzuki R, Maruyama K, Yamashita F, Hashida M. Suppression of Melanoma Growth and Metastasis by DNA Vaccination Using an Ultrasound-Responsive and Mannose-Modified Gene Carrier. Mol Pharm. 8: 543-554 (2011)
14. Negishi Y, Matsuo K, Endo-Takahashi Y, Suzuki K, Matsuki Y, Takagi N, Suzuki R, Maruyama K, Aramaki Y. Delivery of an Angiogenic Gene into Ischemic Muscle by Novel Bubble Liposomes Followed by Ultrasound Exposure. Pharm Res. 28: 712-719 (2011)

15. Hagisawa K, Nishioka T, Suzuki R, Takizawa T, Maruyama K, Takase B, Ishihara M, Kurita A, Yoshimoto N, Ohsuzu F, Kikuchi M. Enhancement of ultrasonic thrombus imaging using novel liposomal bubbles targeting activated platelet glycoprotein IIb/IIIa complex-in vitro and in vivo study. Int J Cardiol., 152: 202-206 (2011)

G-2 学会発表

1. 小俣大樹、鈴木 亮、小田雄介、澤口能一、生井栄佑、根岸洋一、丸山一雄、バブルリポソームと超音波を利用した肝臓への低侵襲的遺伝子導入における特性評価、日本薬学会第133年会、横浜、2013年3月27-30日
2. 小田雄介、鈴木 亮、小俣大樹、澤口能一、根岸洋一、丸山一雄、脳への遺伝子導入効率におよぼすバブルリポソーム構成脂質の影響、日本薬学会第133年会、横浜、2013年3月27-30日
3. 澤口能一、小田雄介、小俣大樹、鈴木 亮、萩沢康介、丸山一雄、超音波、バブルリポソーム併用血栓溶解療法の基礎的検討、日本薬学会第133年会、横浜、2013年3月27-30日
4. 山村 翔、根岸洋一、濱野展人、小俣大樹、奥津大輔、高橋葉子、鈴木 亮、丸山一雄、新槇幸彦、バブルリポソームと高密度焦点式超音波による骨格筋への遺伝子導入法の基礎的検討、アンチセンス・遺伝子・デリバリーシンポジウム2012、仙台、2012年9月24-26日
5. 鈴木 亮、小田雄介、小俣大樹、澤口能一、根岸洋一、丸山一雄、バブルリポソームと超音波を併用したがん組織への遺伝子デリバリー、アンチセンス・遺伝子・デリバリーシンポジウム2012、仙台、2012年9月24-26日
6. 根井彰浩、根岸洋一、高橋佐慧子、小俣大樹、鈴木 亮、丸山一雄、野水基義、新槇幸彦、核移行シグナルペプチド内封 AG73 修飾リポソームによる新規遺伝子デリバリーツールの開発、アンチセンス・遺伝子・デリバリーシンポジウム2012、仙台、2012年9月24-26日
7. 小俣大樹、根岸洋一、鈴木 亮、丸山一雄、野水基義、新槇幸彦、超音波技術を利用したAG73修飾PEGリポソームによる遺伝子導入法の開発、第21回DDSカンファランス、静岡、2012年9月1日
8. Ryo Suzuki, Yusuke Oda, Daiki Omata, Yoshikazu Sawaguchi, Kazuo Maruyama、Enhancement of anti-tumor effect by the combination of ultrasound mediated mild hyperthermia and immunotherapy、ICHO&JCTM 2012、京都、2012年8月28-31日
9. 丸山一雄、小田雄介、小俣大樹、澤口能一、鈴木 亮、バブルリポソームを用いた造影と治療、第28回日本DDS学会、札幌、2012年7月4-5日
10. 根井彰浩、根岸洋一、小俣大樹、山村 翔、高橋葉子、濱野展人、鈴木 亮、丸山一雄、新槇幸彦、バブルリポソームと超音波併用によるペプチド修飾リポソームの遺伝子導入増強効果、日本超音波医学会 第85回学術集会、2012年5月25-27日
11. 鈴木 亮、根岸洋一、必ずうまくいくソノポレーション法:実験の実際とコツ、第4回超音波分子診断治療研究会、福岡、2012年3月3日、招待講演
12. 鈴木 亮、小田雄介、丸山一雄、バブルリポソームと超音波の併用による遺伝子導入特性の評価、マイクバブルと超音波の相互作用に関するシンポジウム、名古屋、2012年1月20日
13. 鈴木 亮、小田雄介、平田圭一、野村鉄也、宇都口直樹、丸山一雄、リポソーム型微小気泡を利用した超音波がん温熱療法と樹状細胞免疫療法の併用によるがん治療効果の増強に関する研究、東京、2011年11月26日
14. Ryo Suzuki, Yusuke Oda, Keiichi Hirata, Tetsuya Nomura, Naoki Utoguchi, Kazuo Maruyama、Development of an effective gene delivery system with sonoporation in cancer gene therapy、AAPS2011、米国、2011年10月22-27日

15. Ryo Suzuki, Tetsuya Nomura, Naoki Utoguchi, Kazuo Maruyama 、Induction of anti-tumor immunity in the combination of therapeutic ultrasound and dendritic cell-based immunotherapy、日本癌学会、名古屋、2011 年 10 月 3-5 日
16. 佐藤紗也佳、真柴拓哉、本田亜紀、Citterio Daniel、小田雄介、鈴木 亮、丸山一雄、鈴木孝治、静岡 DDS カンファランス、静岡、2011 年 9 月 16 日
17. 鈴木 亮、丸山一雄、超音波造影・治療技術の新展開、日本バイオイメージング学会、北海道、2011 年 9 月 1-2 日
18. Ryo Suzuki, Yusuke Oda, Risa Koshima, Keiichi Hirata, Tetsuya Nomura, Naoki Utoguchi, Kazuo Maruyama 、The Combination Therapy of Therapeutic Ultrasound and Dendritic Cell-Based Immunotherapy、WFUMB2011、オーストリア、2011 年 8 月 26-30 日

H. 知的財産権の出願・登録状況

H-1 特許取得

なし

H-2 実用新案登録

なし

H-3 その他

なし

I. 研究協力者

小田 雄介
平田 圭一
宇留賀 仁史
関 むつみ

研究成果の刊行に関する一覧表

書籍

著者氏名	論文タイトル名	書籍全体の編集者名	書 籍 名	出版社名	出版地	出版年	ページ

雑誌

発表者氏名	論文タイトル名	発表誌名	巻号	ページ	出版年
Negishi Y, Hamano N, Shiono H, Akiyama S, Endo-Takahashi Y, Suzuki R, Maruyama K, Aramaki Y.	The development of an ultrasound-mediated nucleic acid delivery system for treating muscular dystrophies.	Yakugaku Zasshi	132	1383-1388	2012
Matsui A, Yokoo H, Negishi Y, Endo-Takahashi Y, Chun NA, Kadouchi I, Suzuki R, Maruyama K, Aramaki Y, Semba K, Kobayashi E, Takahashi M, Murakami T.	CXCL17 expression by tumor cell recruits CD11b+Gr1 high F4/80-cells and promotes tumor progression.	PLoS One	7	e44080	2012
Negishi Y, Endo-Takahashi Y, Matsuki Y, Kato Y, Takagi N, Suzuki R, Maruyama K, Aramaki Y.	Systemic delivery systems of angiogenic gene by novel bubble liposomes containing cationic lipid and ultrasound exposure.	Mol. Pharm.	9	1834-1840	2012
Sonoda S, Tachibana K, Yamashita T, Shirasawa M, Terasaki H, Uchino E, Suzuki R, Maruyama K, Sakamoto T.	Selective gene transfer to the retina using intravitreal ultrasound irradiation.	J. Ophthalmol.	2012	412752	2012
Omata D, Negishi Y, Yamamura S, Hagiwara S, Endo-Takahashi Y, Suzuki R, Maruyama K, Nomizu M, Aramaki Y.	Involvement of Ca2+ and ATP in enhanced gene delivery by bubble liposomes and ultrasound exposure.	Mol. Pharm.	9	1017-1023	2012
Omata D, Negishi Y, Hagiwara S, Yamamura S, Endo-Takahashi Y, Suzuki R, Maruyama K, Aramaki Y.	Enhanced gene delivery using Bubble liposomes and ultrasound for folate-PEG liposomes.	J. Drug Target.	20	355-363	2012

Un K, Kawakami S, Yoshida M, Higuchi Y, Suzuki R, Maruyama K, Yamashita F, Hashida M.	Efficient suppression of murine intracellular adhesion molecule-1 using ultrasound-responsive and mannose-modified lipoplexes inhibits acute hepatic inflammation.	Hepatology	56	259-269	2012
Oda Y, Suzuki R, Otake S, Nishiie N, Hirata K, Koshima R, Nomura T, Utoguchi N, Kudo N, Tachibana K, Maruyama k.	Prophylactic immunization with Bubble liposomes and ultrasound-treated dendritic cells provided a four-fold decrease in the frequency of melanoma lung metastasis.	J. Control. Release	160	362-366	2012
Endo-Takahashi Y, Negishi Y, Kato Y, Suzuki R, Maruyama K, Aramaki Y.	Efficient siRNA delivery using novel siRNA-loaded Bubble liposomes and ultrasound.	Int. J. Pharm.	422	504-509	2012
Sugano M, Negishi Y, Endo-Takahashi Y, Suzuki R, Maruyama K, Yamamoto M, Aramaki Y.	Gene delivery system involving Bubble liposomes and ultrasound for the efficient in vivo delivery of genes into mouse tongue tissue.	Int. J. Pharm.	422	332-337	2012
Omata D, Negishi Y, Hagiwara S, Yamamura S, Endo-Takahashi Y, Suzuki R, Maruyama K, Nomizu M, Aramaki Y	Bubble Liposomes and Ultrasound Promoted Endosomal Escape of TAT-PEG Liposomes as Gene Delivery Carriers	Mol Pharm	8	2416-2423	2011
Un K, Kawakami S, Higuchi Y, Suzuki R, Maruyama K, Yamashita F, Hashida M	Involvement of activated transcriptional process in efficient gene transfection using unmodified and mannose-modified bubble lipoplexes with ultrasound exposure.	J Control Release	156	355-363	2011
Shiraishi K, Endoh R, Furuhata H, Nishihara M, Suzuki R, Maruyama K, Oda Y, Jo J, Tabata Y, Yamamoto J, Yokoyama M	A facile preparation method of a PFC-containing nano-sized emulsion for theranostics of solid tumors	Int J Pharm	421	379-387	2011

Un K, Kawakami S, Suzuki R, Maruyama K, Yamashita F, Hashida M.	Suppression of Melanoma Growth and Metastasis by DNA Vaccination Using an Ultrasound-Responsive and Mannose-Modified Gene Carrier	Mol Pharm	8	543-554	2011
Negishi Y, Matsuo K, Endo-Takahashi Y, Suzuki K, Matsuki Y, Takagi N, Suzuki R, Maruyama K, Aramaki Y.	Delivery of an Angiogenic Gene into Ischemic Muscle by Novel Bubble Liposomes Followed by Ultrasound Exposure	Pharm Res	28	712-719	2011
Hagisawa K, Nishioka T, Suzuki R, Takizawa T, Maruyama K, Takase B, Ishihara M, Kurita A, Yoshimoto N, Ohsuzu F, Kikuchi M.	Enhancement of ultrasonic thrombus imaging using novel liposomal bubbles targeting activated platelet glycoprotein IIb/IIIa complex-in vitro and in vivo study	Int J Cardiol	152	202-206	2011

International Journal of Pharmaceutics 421 (2011) 379–387

Contents lists available at SciVerse ScienceDirect

International Journal of Pharmaceutics

journal homepage: www.elsevier.com/locate/ijpharm

A facile preparation method of a PFC-containing nano-sized emulsion for theranostics of solid tumors

Kouichi Shiraishi[a], Reiko Endoh[a], Hiroshi Furuhata[a], Masamichi Nishihara[b], Ryo Suzuki[c], Kazuo Maruyama[c], Yusuke Oda[c], Jun-ichiro Jo[d], Yasuhiko Tabata[d], Jun Yamamoto[e], Masayuki Yokoyama[a,*]

[a] Medical Engineering Laboratory, Research Center for Medical Science, The Jikei University School of Medicine, 3-25-8, Nishi-shinbashi, Minato-ku, Tokyo 105-8461, Japan
[b] International Institute for Carbon-Neutral Energy Research (I²CNER), Kyushu University, 744 Motooka, Nishi-ku, Fukuoka 819-0395, Japan
[c] Department of Biopharmaceutics, School of Pharmaceutical Sciences, Teikyo University, 1091-1 Suwarashi, Midori-ku, Sagamihara, Kanagawa 252-5195, Japan
[d] Department of Biomaterials, Institute for Frontier Medical Sciences, Kyoto University, 53 Kawara-cho Shogoin, Sakyo-ku, Kyoto 606-8507, Japan
[e] Division of Physics and Astronomy, Graduate School of Science, Kyoto University, Kitashirakawa Oiwake-cho, Sakyo-ku, Kyoto 606-8502, Japan

ARTICLE INFO

Article history:
Received 14 June 2011
Received in revised form 27 August 2011
Accepted 2 October 2011
Available online 15 October 2011

Keywords:
Theranostics
Tumor targeting
Ultrasound
Perfluorocarbon
Emulsion

ABSTRACT

Theranostics means a therapy conducted in a diagnosis-guided manner. For theranostics of solid tumors by means of ultrasound, we designed a nano-sized emulsion containing perfluoropentane (PFC5). This emulsion can be delivered into tumor tissues through the tumor vasculatures owing to its nano-size, and the emulsion is transformed into a micron-sized bubble upon sonication through phase transition of PFC5. The micron-sized bubbles can more efficiently absorb ultrasonic energy for better diagnostic images and can exhibit more efficient ultrasound-driven therapeutic effects than nano-sized bubbles. For more efficient tumor delivery, smaller size is preferable, yet the preparation of a smaller emulsion is technically more difficult. In this paper, we used a bath-type sonicator to successfully obtain small PFC5-containing emulsions in a diameter of ca. 200 nm. Additionally, we prepared these small emulsions at 40 °C, which is above the boiling temperature of PFC5. Accordingly, we succeeded in obtaining very small nano-emulsions for theranostics through a very facile method.

1. Introduction

'Theranostics', 'theranosis', or 'theragnosis' is a newly created term in the fields of imaging diagnosis and drug delivery systems. As a word, 'theranostics' (Chen, 2011; Lammers et al., 2010, 2011; MacKay and Li, 2010) is a combination of therapy and diagnosis, and is defined as therapy conducted in a diagnosis-guided manner. A typical example of theranostics is found in a carrier system containing both a contrast agent for diagnosis and a drug for therapy. Theranostics has been studied with various types of drug carriers including liposomes (Kamaly and Miller, 2010), small molecules (Kalber et al., 2011), nano-particles (Jeong et al., 2011; Kim et al., 2010), emulsions (Gianella et al., 2011), synthetic polymers (Bryson et al., 2009), polymeric micelles (Blanco et al., 2009; Kaida et al., 2010; Min et al., 2010; Nakamura et al., 2006; Shiraishi et al., 2009, 2010), and other nano-sized carrier systems (Ai, 2011; Moon et al., 2011; Pan et al., 2008; Sanson et al., 2011). Ultrasound is considered to be a preferable modality for theranostics because ultrasound has been well studied and developed for image diagnoses and local therapies such as ultrasound lithotresis and hyperthermia.

For theranostics of solid tumors, micron-sized bubbles (microbubbles) (Hernot and Klibanov, 2008; Schutt et al., 2003; Unger et al., 2004) have been actively studied because the bubbles provide strong contrasts in ultrasonic images, and because cavitation of microbubbles (Grishenkov et al., 2009) induced by ultrasound can effectively damage cells. Cells can be damaged by both jet-stream and heat that are generated in the bubbles' cavitation. In the design of microbubbles for tumor applications, the size of the microbubbles is a very important factor. Larger microbubbles can produce stronger ultrasound image contrasts. In contrast, smaller bubbles are preferred for efficient delivery into tumor tissues because the size of the trans-vascular passage from the bloodstream into the tumor interstitial space is of a diameter smaller than 1 μm. It is believed that the maximum diameter for efficient translocation into tumor tissues is 200–400 nm (Ishida et al., 1999; Litzinger et al., 1994; Nagayasu et al., 1996; Yuan et al., 1995). (In this diameter range, bubbles must be called nano-bubbles.) This is an essential dilemma concerning the size of bubbles used for

Abbreviations: PFC, perfluorocarbon; PFC5, perfluoropentane; PFC6, perfluorohexane; DBU, 1,8-diazabicyclo[5.4.0]undec-7-ene; PEG-P(Asp(C7F9)x), poly(ethylene glycol)-b-poly(4,4,5,5,6,6,7,7,7-nonafluoroheptyl aspartate) block copolymer.

* Corresponding author. Tel.: +81 3 3433 1111x2336; fax: +81 3 3459 6005.
E-mail address: masajun2093ryo@jikei.ac.jp (M. Yokoyama).

0378-5173/$ – see front matter © 2011 Elsevier B.V. All rights reserved.
doi:10.1016/j.ijpharm.2011.10.006

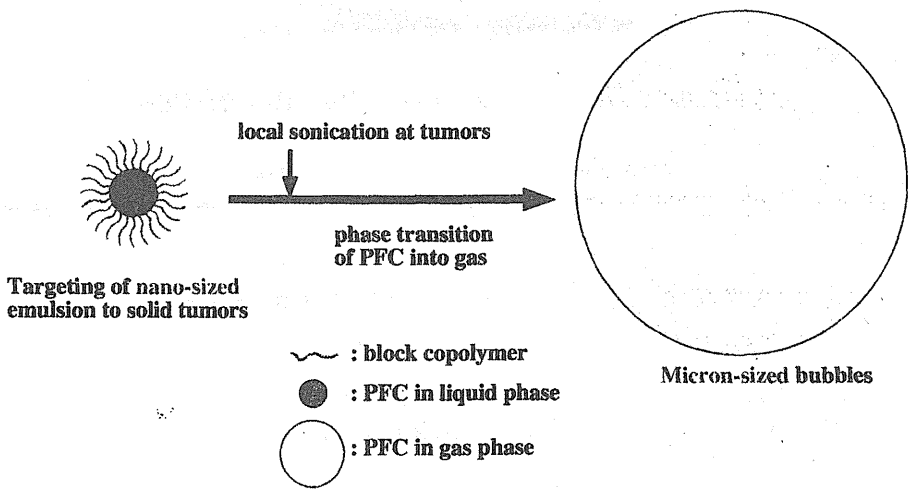

Fig. 1. Concept of phase-transition type nano-emulsion.

tumor theranostics. In order to resolve this dilemma, Kawabata et al. (Asami et al., 2009, 2010; Kawabata et al., 2005, 2010a,b) and Rapoport et al. (Mohan and Rapoport, 2010; Rapoport et al., 2007, 2009a, 2009b, 2010a,b, in press) examined nano-emulsions incorporating a specific kind of perfluorocarbon, as illustrated in Fig. 1. A boiling temperature of this perfluorocarbon (perfluoropentane, PFC5) is 29 °C, which is lower than normal human body temperature, but the integrity of these nano-emulsions is maintained owing to interfacial excessive pressure called Laplace pressure (Rapoport et al., 2009a). Upon ultrasound irradiation, the integrity of these nano-emulsions is broken, and this liquid perfluorocarbon exhibits a phase-transition into gas. Accordingly, the nano-emulsions change into microbubbles. Efficient delivery into tumor tissues is attained with the nano-emulsions, and then local sonication at the tumor tissues generates the microbubbles from the nano-emulsions, resulting in high imaging and therapeutic efficiencies. This phase-transition type nano-emulsion may be an ideal system for the theranostics of solid tumors.

Generally, preparations of smaller emulsions in a nano-meter range are more difficult because a higher power input is required in the emulsion preparations. (Tadros et al., 2004) Previously, we had prepared perfluorocarbon-containing emulsions by means of vigorous mechanical stirring with a magnetic stirrer and obtained emulsions of ca. 600 nm in diameter (Nishihara et al., 2009). In this paper, we have tried to obtain much smaller emulsions by means of ultrasound irradiation as well as high-pressure emulsification. Another important parameter for preparations of the phase-transition type nano-emulsion is temperature. A boiling temperature (29 °C) of perfluoropentane (PFC5) is close to the room temperature; therefore, preparations must be carried out at a low temperature and in a small scale for evasion of evaporation of PFC5 because heat generated in emulsification or sonication processes must be efficiently removed for the evasion. We want to find a facile preparation method that can be carried out at either room or a higher temperature, and that can be easily scaled up because the heat removal is a much less serious concern than the conventional method. Rapoport et al. (Rapoport et al., 2010b) reported preparations of nano-bubbles by means of ultrasound irradiation (with a probe type sonicator at 20 kHz) in ice-cold water. They obtained nano-emulsions of ca. 600 nm in diameter.

In this paper, we have tried to obtain very small nano-emulsions containing PFC5 by using an inexpensive bath-type sonicator (usually used as an ultrasonic cleaner) at room temperature or higher. For this emulsion preparation, we synthesized fluorinated block copolymers and optimized their compositions.

2. Materials and methods

2.1. Materials

We purchased perfluoropentane (PFC5) and perfluorohexane (PFC6) from Stream Chemicals (Newburyport, MA, USA) and Alfa Aesar (Ward Hill, MA, USA), respectively, and used them as received. We purchased 4,4,5,5,6,6,7,7,7-nonafluoroheptyl iodide from Sigma–Aldrich (Tokyo branch, Japan) and used it as received. We purchased reagent-grade solvents, dehydrated *N,N*-dimethylformamide (DMF), dimethyl sulfoxide (DMSO), and diethyl ether from Wako Chemicals (Tokyo, Japan), and used them as received. Poly(L-lactic acid)-grafted gelatin was prepared through a coupling reaction between a primary amine group of gelatin and a terminal hydroxyl group of the poly(L-lactic acid) by the use of disuccimidyl carbonate according to a published synthetic procedure. (Tanigo et al., 2010) Poly(ethylene glycol)-block-poly(L-lactic acid) block copolymer (PEG-b-PLA) was purchased from Sigma–Aldrich (Tokyo branch, Japan). The average molecular weights of the PEG block and the PLA block were 750 and 1,000, respectively.

2.2. Block copolymer synthesis

Poly(ethylene glycol)-*b*-poly(4,4,5,5,6,6,7,7,7-nonafluoroheptyl aspartate) block copolymers (PEG-P(Asp(C7F9)*x*)) were prepared by means of esterification of the aspartic units of poly(ethylene glycol)-b-poly(aspartic acid) block copolymer (PEG-P(Asp)) by the use of an iodinated compound, as shown in Fig. 2. PEG-P(Asp) was synthesized according to our previous paper (Yamamoto et al., 2007). A value *x* in the PEG-P(Asp(C7F9)*x*) formula denotes mol.% of the esterified units. This esterification reaction was carried out with a corresponding iodinated compound in the presence of a super base according to a previously reported procedure (Opanasopit et al., 2004; Yokoyama et al., 2004; Yamamoto et al., 2007) with a slight modification.

The starting material was poly(ethylene glycol)-b-poly(aspartic acid) block copolymer (PEG-P(Asp)). The average molecular weight of PEG was 5200 (n=119 in Fig. 2), and the average number of Asp units per one chain was 26.0. The aspartate amide bond can be either α or β, and our group previously had reported that a ratio of α:β was 1:3 (=*a*:*b* in Fig. 2) (Yokoyama et al., 2004). PEG-P(Asp) (2.001 g, containing 6.33×10^{-3} mol Asp residue) was dissolved in 20 mL of DMF. To this mixture, was added both 4.904 g of 4,4,5,5,6,6,7,7,7-nonafluorohepty iodide (which is

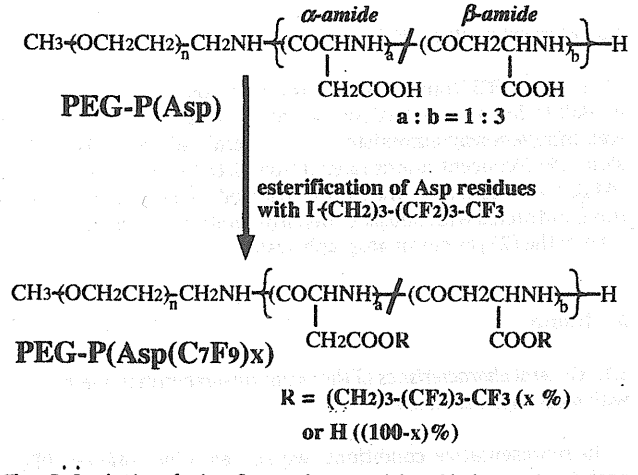

Fig. 2. Synthesis of the fluorocarbon-containing block copolymer PEG-P(Asp(C7F9)x).

2.00 mol. equivalents to the Asp residue, I-(CH2)3-(CF2)3-CF3 in Fig. 2) and 0.972 g of 1,8-diazabicyclo[5.4.0]undec-7-ene (DBU, which is 1.01 mol. equivalents to the Asp residue). DBU is a very strong base, and can induce ionization in a carboxyl group of the aspartic acid residue in an organic solvent, DMF. The reaction mixture was heated at 50 °C for 16 h. An ester formed at the Asp residue through a nucleophilic substitution reaction of the ionized carboxyl group with I-(CH2)3-(CF2)3-CF3. After this 16-h reaction, the reaction mixture was poured into 200 mL of ice-cold diethyl ether for precipitation of the polymer. The precipitated polymer was filtered and washed with diethyl ether. The obtained polymer was dissolved in 20 mL of DMSO, to which was added 2.11 mL of 6 N hydrochloric acid. This acid works for removal of DBU from polymers. This polymer solution was dialyzed with a Spectra/Por 6 dialysis membrane (molecular weight cut-off is 1000) against DMSO for 2 days and against milliQ water for an additional 2 days, followed by freeze-drying. Yield was 2.436 g. To determine the contents of the fluorinated ester group of the polymer, we used ^{1}H NMR spectroscopy in DMSO-d_6 containing 3 v/v% trifluoroacetic acid. For this determination, we identified a peak area ratio between the methylene protons ($-COOCH_2\underline{CH_2}CH_2CF_2CF_2CF_2CF_3$) at 1.8 ppm of the ester group and the methylene protons ($-OC\underline{H_2}\underline{CH_2}-$) at 3.6 ppm of the PEG block. The esterification percentage (x in Fig. 2) was revealed to be 59%. The other compositions of block copolymers were synthesized according to the same method with various molar ratios of I-(CH2)3-(CF2)3-CF3 and DBU with respect to the aspartic acid residue. Table 1 lists all the compositions of the synthesized block copolymers.

Table 1
Compositions of PEG-P(Asp(C7F9)x).

Code	M.W. of PEG	Asp unit number (n)	Esterification degree (x%)
F-6%	5200	22.1	5.9
F-15%	5200	23.3	14.6
F-39%	5200	22.1	38.5
F-59%	5200	26.0	58.5
F-67%	5200	22.1	67.0

2.3. Preparation of PFC-containing nano-emulsions

We examined preparations of PFC5-containing nano-emulsions according to two methods using a high-pressure emulsifier and a bath-type sonicator.

2.3.1. Preparation with a high-pressure emulsifier

We dissolved PEG-P(Asp(C7F9)15) block copolymer by stirring it in distilled water at a concentration of 4.0 wt. % of the solution, and added perfluoropentane (PFC5) and perfluorohexane (PFC6) at each 1.25 vol.% of the solution. We vigorously stirred the solution with a homogenizer Polytron (Kinematica AG, Tokyo, Japan) at 25,000 rpm for 10 s. Then, we conducted emulsification using a high-pressure emulsifier EmulsiFlex-C5 CSC (AVESTIN, Inc., Ottawa, Ontario, Canada) at 4 °C for 6 min at ca. 50 MPa. We collected a white emulsion, and filtered it with a Sartorius Minisart (R) filter (1.2 μm pore, Sartorius AG, Göttingen, Germany).

2.3.2. Preparation with a bath-type sonicator

We dissolved PEG-P(Asp(C7F9)x) block copolymers in MilliQ water at a concentration of 1.0 to 4.0 wt.% of water. In case of a high ester content such as x = 59, we heated (up to ca. 40 °C) and sonicated the solutions until we obtained a transparent polymer solution. The polymer solution was transferred to a 1.5-mL glass vial that was sealed with a Teflon–silicon rubber cap (Chromacol auto-sampler vial 2-SV for HPLC; GL Science, Inc., Tokyo, Japan), and was cooled on ice. Then, we added perfluoropentane (PFC5) and perfluorohexane (PFC6) at 0.5–4.0 vol.% of water. We confirmed PFCs' position at the bottom of the solution. (Sometimes PFCs, whose densities are much greater than water's, did not go into the aqueous solution. Therefore, we shook the vial vigorously to allow PFC droplets to sink to the bottom by force of gravity.) Then, we sealed the vial with a cap, and applied sonication for 3 min with a bath-type sonicator Branson model 1510 (oscillating frequency at 42 kHz, max. power intensity: 90 W, Danbury, CT, USA). The temperature of the bath was kept constant with degassed cold and hot water. In all the sonication procedures, we had a constant water level in a sonicator bath and a fixed position of the vial in order to obtain sonication conditions that were as identical to one another as possible. Finally, we collected a supernatant by leaving unincorporated PFC droplets at the bottom.

Table 2
Effects of polymer composition and sample volume on PFC5 incorporation behaviors.

Run	Polymer	Sample volume (μL)	PFC5 concentration (vol.%)[a]	Cumulant average diameter (nm)[a]
1	F-6%	300	0.840 ± 0.097	261.2 ± 3.4
2	F-15%	300	0.948 ± 0.131	232.4 ± 14.5
3	F-39%	300	0.625 ± 0.074	198.4 ± 33.3
4	F-59%	300	0.669[b]	133.9[b]
5	F-67%	300	0.682 ± 0.060	222.8 ± 37.9
6	F-59%	300	0.682 ± 0.074	205.5 ± 15.8
7	F-59%	300	0.634 ± 0.361	173.5 ± 24.5
8	F-59%	700	1.110[b]	231.8[b]
9	F-59%	1200	1.792[b]	280.6[b]

[a] Average ± standard deviation (n = 3) except runs 4, 8, and 9.
[b] Average of two preparations.

In order to measure amounts of the polymer chains that were not included in the PFC-emulsions, we carried out the following experiment. PFC-emulsion was prepared in the conditions of Run 4 of Table 2; polymer: F-59%, sample volume: 300 μL, polymer concentration: 4 wt.%, PFC5: 2 vol.%, PFC6: 2 vol.%, sonication at 40 °C for 3 min. The obtained emulsion was transferred into a 1.5 mL Eppendorf-type poly(propylene) tube and centrifuged at 13,200 rpm for 5 min with an Eppendorf centrifuge model 5415D (Eppendorf Co., Ltd. Japan, Tokyo, Japan). The emulsion was found to precipitate at the bottom. 200 μL of the supernatant was collected and freeze-dried. We calculated the polymer amounts that were not included in the PFC-emulsions by multiplying 1.5 (=300 μL/200 μL) to the freeze-dried polymer weight. As a control, we carried out the same experiment just only for the polymer (without addition of TFC5 nor TFC6).

2.4. Measurements

2.4.1. Dynamic light scattering (DLS)

The size of emulsions was measured with a dynamic light scattering (DLS) instrument, the DLS-7000 (Otsuka Electronics, Tokyo, Japan). DLS samples were prepared through appropriate dilution of the emulsions with commercial distilled water for internal injection (Otsuka Pharmaceutical Co. Ltd., Tokyo, Japan). The measurements were made at 25 °C, and scattering was observed at a 90° angle with respect to the incident beam. The cumulant average particle size and the particle size distribution from a non-negative least square method were determined by the use of software provided with the instrument.

2.4.2. Gas chromatography

We measured concentrations of PFC5 using two gas chromatograph systems as described below. In both cases, we successfully obtained clear separation of PFC5's peak from PFC6's peak, and carried out quantitative analyses using a standard sample of PFC5. Therefore, the two gas chromatograph systems gave us identical results. However, we only used the (2) system described below for blood samples because its pre-heating function was essential for measurements of blood samples.

2.4.2.1. Gas chromatograph system. We measured PFC5 using a gas chromatograph model G-6000 (Hitachi High-Technologies Corporation, Tokyo, Japan) equipped with a Gaskuropack 54 80/100 packed column (GL Sciences, Inc., Tokyo, Japan) and an FID detector at 200 °C. Carrier gas was nitrogen at a flow rate of 300 mL/min. 5 μL of a sample solution were injected into the gas chromatograph system with a micro syringe at 0 min. Column temperature was controlled in the following manner; 100 °C (0 min), raised at a rate of 5 °C/min until 130 °C (6 min), and then raised at a rate of 60 °C/min until 190 °C (7 min), followed by maintenance of 190 °C for 2 min. PFC5 and PFC6 were found to elute at 3.8 min and 6.4 min, respectively.

2.4.2.2. Gas chromatograph system. We measured PFC5 using a gas chromatograph system GC-2014 (Shimadzu Corp., Kyoto, Japan) equipped with an FID detector at 250 °C. We used two tandem-connected two columns: DB-WAX 127-7012 (Agilent Technologies Japan, Ltd., Tokyo, Japan) and RESTEK Rt-QBond 19741 (Shimadzu GLC Ltd., Tokyo, Japan). Carrier gas was helium at a flow rate of 20 mL/min. Either 100 or 544 μL of a sample solution were heated at 200 °C and injected with a headspace autosampler TurboMatrix Trap 40 (PerkinElmer Japan Co., Ltd., Yokohama, Japan). Column temperature was constant at 150 °C. PFC5 and PFC6 were found to elute at 3.6 min and 4.4 min, respectively.

2.5. Measurements of PFC5 concentration in blood

In vivo PFC5 concentration profiles in blood were evaluated in Balb/c female mice (6 weeks old). 100 μL of PFC-emulsion was intravenously administered via lateral tail veins. The emulsions' PFC5 concentrations ranged from 0.429 to 0.670 vol.%. Blood (44 μL) was collected with a heparinized blood-collecting glass tube, and mixed with 500 μL of heparin solution in a capped sample tube of the (2) gas chromatograph system.

3. Results

3.1. General characteristics of the emulsion-preparation method with a bath-type sonicator

In representative conditions, we successfully obtained PFC5-containing nano-sized emulsions having diameters of ca. 200 nm in considerably high PFC5 yields. Fig. 3(a) and (b) shows diameter distributions measured by means of dynamic light scattering (DLS) for PEG-P(Asp(C7F9)59) (F-59% in Table 1). In these conditions, we dissolved 12.0 mg of polymer in 300 μL water (4.0 wt.% solution), and put this polymer solution in a 1.5 mL glass vial, followed by additions of 6 μL (corresponding to 2.0 vol.% of water) of PFC5 and 6 μL of PFC6. Sonication was performed for 3 min in a bath-type sonicator at 40 °C. In the first three preparations (run 6 in Table 2), the cumulant diameter obtained was 205.5 ± 15.8 nm (the average ± standard deviation; $n = 3$), and Fig. 3(a) shows the weight-weighted diameter distribution of one preparation. Almost uniformly distributed emulsions were obtained, and the diameter of the emulsion droplets had a very small size about 200 nm. In this run 6, PFC5 concentrations were 0.682 ± 0.074 vol.%. These values are considered large enough for ultrasound images (Kawabata et al., 2005, 2010a,b). In another set of three preparations (on another day, run 7 in Table 2), we obtained a very similar average diameter, 173.5 ± 24.5 nm (the average ± standard deviation; $n = 3$) and PFC5 concentrations. The diameter distribution of one preparation of run 7 is shown in Fig. 3(b). These two figures exhibited a major peak at about 200 nm, while a minor peak was seen in a larger diameter side and a smaller diameter side, as shown in Fig. 3(a) and (b), respectively. This difference may result from a slight variation in sonication conditions such as the position of samples and the water level of the sonicator. These emulsions were obtained and measured without any purification process after the sonication, and a large majority of the emulsions in weight were found to have a diameter of about 200 nm. All these results clearly indicate that this sonication method brought about very small nanometer-sized PFC5-containing emulsions with considerably high PFC5 concentrations.

We measured a proportion of polymer incorporated in the PFC-emulsion out of the feed polymer amount. In these preparation conditions (run 7 in Table 2), 75.4 ± 2.6% ($n = 3$) of the feed polymer was found in a supernatant obtained after centrifugation. (All the PFC-emulsions were observed to precipitate in this centrifugation.) When this measurement was carried out for the polymer alone, 93.8 ± 2.0% ($n = 3$) of the feed polymer was found in a supernatant obtained after centrifugation. Therefore, 18.4% (=93.8%–75.4%) of the feed polymer was considered to be incorporated into the PFC-emulsions. Removal of the free polymer chain, that was not incorporated into the PFC-emulsion, was not examined in this study. The removal is difficult because the free polymer existed as a polymeric micelle was close to the PFC-emulsion in size. (If the free polymer existed as a single polymer chain, a difference in size between the free polymer and the PFC-emulsion would be so large to allow separation such as ultrafiltration.)

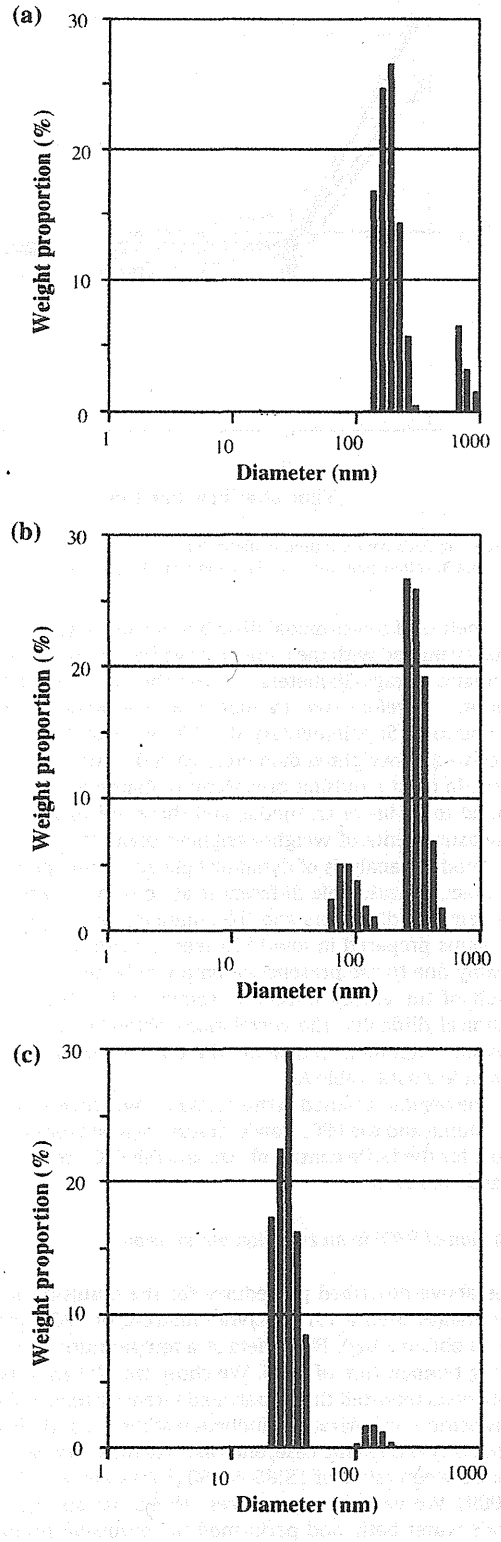

Fig. 3. Diameter distribution of PFC5-containing nano-emulsions (a and b) forming from PEG-P(Asp(C7F9)59) and empty polymeric micelle (c) measured by means of DLS. (a and b) are of different batches but prepared in the same conditions.

Using this polymer amount incorporated into the PFC-emulsions, we calculated the thickness of the polymer shell. We carried out the calculation with the following assumptions.

(1) The PFC-emulsions are made of the two phases; the inner PFC droplet phase and the outer polymer shell phase.
(2) We obtained PFC6 amounts in the emulsions assuming that sensitivity of PFC6 in gas chromatography is the same as that of PFC5. (The same peak area per PFC volume.)
(3) PFC6 and PFC5 are mixed freely without any gain or loss of droplet volume.
(4) Density of polymer is 1.03. (This is a common value of protein, and most synthetic polymers show similar values.)

The obtained value of the polymer shell's thickness was 22 nm, while the radius of the PFC droplet was 65 nm. In the future study, we like to analyse relationships between the shell thickness and physical stability of the emulsions.

3.2. Comparison with other emulsion-preparation methods

We compared the PFC5's concentrations of the PFC5-containing emulsions prepared in the sonication method with the PFC5's concentrations of the emulsions prepared in two common methods; mechanical stirring and high-pressure emulsification (Solans et al., 2005). We also compared the diameters of the emulsions prepared in the sonication method with those prepared in the two common methods. Previously, we reported PFC5-containing emulsions prepared by means of mechanical stirring that featured a magnetic stirrer (Nishihara et al., 2009). In this method, only the F-14% polymer provided a high PFC5 concentration (0.65 vol.%). The other polymers provided low or very low PFC5 concentrations: F-6% had 0.28 vol.%, F-22% had 0.19 vol.%, F-39% had 0.02 vol.%, and F-67% had 0.01 vol.%. In the F-14% case, the cumulant diameter was 694 nm, which was much larger than those obtained in the sonication method as described in the previous section (Section 3.1). Another distinct difference was found in a wide range of polymer compositions for high PFC5 concentrations in the sonication method. As summarized in runs 1–5 of Table 2, we compared the PFC5 concentrations (vol.%) and average diameters of the PFC5-containing emulsions for five polymer compositions. All these five compositions of polymers provided high PFC5 concentrations larger than 0.6 vol.%. Furthermore, all emulsion sizes of these runs (runs 2–5) were revealed to be small, at about 200 nm.

In the next step, we compared the sonication method with the most common method for emulsion preparation: high-pressure emulsification. For this comparison, we used F-15% polymer. We compared PFC5 concentrations and the cumulant average diameters of the emulsions prepared in the sonication method with PFC5 concentrations and the cumulant average diameters of the "high-pressure method" emulsions. We acquired a considerably high PFC5 concentration, 0.58 vol.%, by using a high-pressure emulsifier for the high-pressure emulsification method (its procedure is described in Section 2.3.1). However, the cumulant average diameter of the obtained emulsion was 477 nm. This value was much larger than the sonication-method value (232.4 nm, run 2 of Table 2). Additionally, maintenance of a low temperature at 4 °C for the whole instrument was essential in the high-pressure emulsification method, since possible heat generation due to the high-pressure process may considerably boost evaporation of PFC5 (the boiling temperature of PFC5 is 29 °C). In contrast, in the sonication method, a high PFC5 concentration was obtained at 40 °C, which is above PFC5's boiling temperature. (The temperature issue of the emulsion-preparation process will be more closely examined in the following section (Section 3.4).)

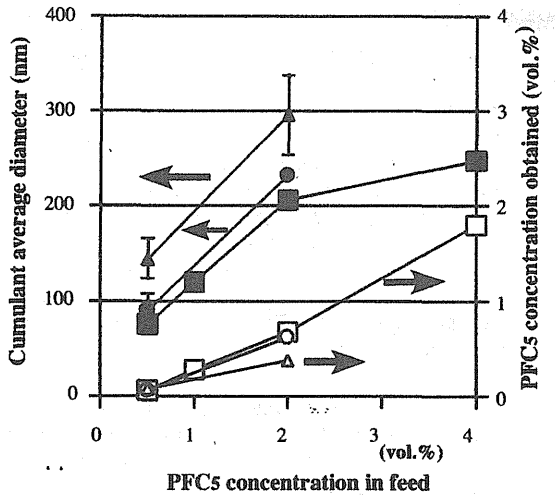

Fig. 4. Effects of polymer and PFC5 concentrations on physical properties of emulsions. PEG-P(Asp(C7F9)59) was used for emulsion preparations. Sample volume was 300 μL in 1.5-mL sample vials. Sonication was performed for 3 min at 40 °C. Filled plots represent cumulant average diameters, and vacant plots represent PFC5 concentrations of emulsions. Polymer concentration: △, ▲: 1.0 vol.%; ○, ●: 2.0 vol.%; □, ■: 4.0 vol.%.

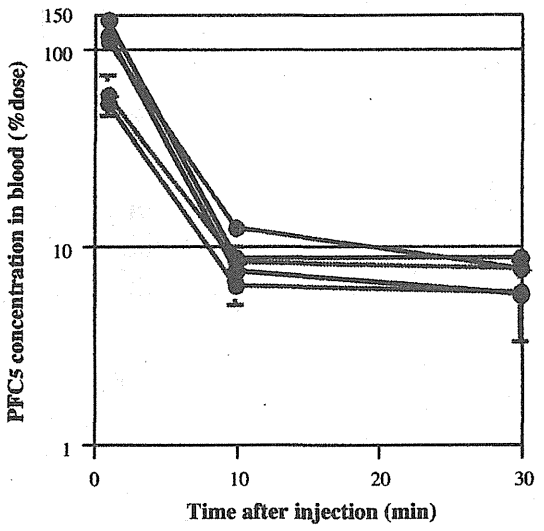

Fig. 5. Profiles of PFC5 concentration in blood. Black plot: run 1; blue plot: run 2; green plot: run 3; yellow plot: run 4; and red plot: run 5 (Table 5).

All these results indicate that the sonication method is a facile method for preparations of PFC5-containg emulsions with very small nano-sizes and high PFC5 concentrations.

3.3. *Effects of sample volume, polymer concentration, and PFC5 concentration on incorporation behaviors*

In the standard conditions, we put 300 μL water in a 1.5-mL of sealed glass tube and added polymer, PFC5, and PFC6. This configuration meant that a considerable amount of PFC5 perhaps would move from the solution into the glass tube's vacant atmospheric space (ca. 1.2 mL). We changed the volume of water while keeping constant the concentrations of polymer, PFC5, and PFC6 in the tube. Table 2 summarizes the results of runs 6–9 of Table 2. A higher PFC5 concentration was obtained in a case involving a larger water volume. (This means that there was a smaller vacant space in a sealed tube.) In accordance with the higher concentration of PFC5, the average diameter of the emulsion was observed to be larger. In run 9, PFC5's yield reached a very high value, approximately 90%. On the other hand, the PFC5's yield decreased to 32–33% when a small sample volume (300 μL) was adopted. These values indicate that the emulsification process can be well controlled through adjustment of sample volume.

Then, we examined effects that both polymer concentrations and PFC5 concentrations in feed had on the two physical values: diameter and PFC5 concentrations of the emulsion. Fig. 4 shows results of these two physical values for F-59% polymer cases. We changed the polymer concentration and the PFC5 concentration in feed in a range of 1.0–4.0 wt.% and of 0.5–4.0 vol.%, respectively. Each empty plot indicates PFC5 concentrations obtained for each polymer concentration, while each filled plot indicates cumulant average diameters for each polymer concentration. The polymer concentration was not found to significantly affect these two physical values. The polymer concentration affected very slightly the PFC5 content because three plot lines almost overlapped. When the polymer concentration was raised, only a small drop in the cumulant average diameter was observed. In contrast, the PFC5 concentration in feed was revealed to greatly affect the two physical values; larger values of PFC5 concentrations and cumulant average diameters were obtained with larger PFC5 concentrations in feed. Diameters of multi-modal distributions like Fig. 3(a) and (b) cannot be evaluated with the cumulant average diameters because the cumulant average diameters suppose the uni-modal diameter distribution. Therefore, we evaluated weight-weighted diameter distributions. Supplementary data, Table A summarizes and compares weight-weighted diameters with the cumulant average diameters. In most emulsion preparations, diameter distributions were found to be bi- or tri-modal, and therefore, exactly quantitative measurements of weight-weighted diameters are difficult in the homodyne analysis of dynamic light scattering done in this study. In fact, considerable differences are observed between the weight-weighted diameters and the cumulant average diameters for emulsions prepared in low PFC5 feed concentrations such as 1%, possibly due to the presence of empty polymeric micelles. (A DLS result of the empty micelle is shown in Fig. 3(c).) Even in this technical difficulty, the correlations obtained in Fig. 4a are not changed when multi-modal distributions are compared in the Supplementary data, Table A.

From the results obtained in this section, it was revealed that the sample volume and the PFC5 concentration in feed were appropriate factors for the facile control of size and the PFC5 content of the nano-sized emulsion.

3.4. *Function of PFC6 in an emulsion preparation*

In the above-described procedures for the emulsion preparation, we always used a 1:1 (vol./vol.) mixture of PFC5 and PFC6 in order to obtain a high PFC5 yield at a temperature higher than the boiling temperature of PFC5. We chose this 1:1 ratio because Kawabata et al. reported that ultrasound intensity required for the phase-transition (vaporization) induction at the 1:1 ratio was similar to that of a PFC5 alone case, and that this intensity was almost constant between ratios of 15:85, 50:50 (=1:1), and 85:15 (Asami et al., 2009). We varied temperatures (15, 25, 40, and 65 °C) of a sonicator's water bath, and performed the emulsion preparation both in the presence and the absence of PFC6 at each temperature. Table 3 summarizes results. In the absence of PFC6, PFC5 concentration was smaller than that of the corresponding PFC6-present case at every temperature. In runs 2 and 4, the obtained emulsions contained a considerable quantity of PFC5 over 0.2 vol.%. These two runs were prepared at lower temperatures than a boiling temperature of PFC5 (29 °C). Only a very small amount of PFC5

Table 3
Effects of temperature and PFC6 addition on PFC5 incorporation behaviors.

Run	Temperature (°C)	PFC6 addition	PFC5 concentration (vol.%)[a]	Cumulant average diameter (nm)[a]
1	15	Yes	0.727 ± 0.191	210.8 ± 17.8
2	15	No	0.419 ± 0.124	82.7 ± 2.6
3	25	Yes	0.566 ± 0.367	177.1 ± 8.9
4	25	No	0.205 ± 0.086	95.7 ± 8.9
5[b]	40	Yes	0.634 ± 0.361	173.5 ± 24.5
6	40	No	0.049 ± 0.059	98.5 ± 5.1
7	65	Yes	0.154 ± 0.051	136.2 ± 16.0
8	65	No	0.096[c]	303.7[c]

[a] Average ± standard deviation ($n = 3$) except run 8.
[b] This run is identical to run 6 of Table 2.
[c] Average of two preparations.

was incorporated in run 6, which was performed at 40 °C, which is above PFC5's boiling temperature. This indicates that most PFC5 evaporated at 40 °C, and that interfacial Laplace pressure did not suppress PFC5's evaporation in the sonication procedure possibly because PFC5 evaporated from macroscopic PFC's droplets (in mm scale) before its incorporation into nano-emulsions where Laplace pressure's effect is great. In contrast, the PFC6-present cases presented similar amounts of PFC5 incorporated at 15, 25, and 40 °C. This means that PFC5's evaporation at 40 °C was efficiently suppressed through the mixing with PFC6. PFC5 and PFC6 not only are miscible but also these two compounds are expected to strongly interact with each other because these are both perfluorocarbons. It is considered that PFC5 evades evaporation through the strong interaction with PFC6 that has a higher boiling temperature than 40 °C. In run 7, performed at 65 °C, a considerable drop in the incorporated PFC5 amount was seen. This sonication temperature (65 °C) is higher than PFC6's boiling temperature (60 °C), and therefore, both PFC5 and PFC6 were evaporated at 65 °C. From these results, we have confirmed the function of the added PFC6 for high PFC5-incorporation amounts at a temperature higher than PFC5's boiling temperature.

3.5. PFC5 concentration profile in blood

We measured PFC concentrations in blood using several PFC5-containing emulsions in order to control their pharmacokinetic behaviors. For a larger amount of emulsion accumulation at tumor tissues, a longer half-life is preferable for a contrast agent. In contrast, a shorter half-life is advantageous for a diagnosis in a short period after injection of a contrast injection, since a low concentration of the contrast agent in blood is a pre-requisite for a high contrast image of the contrast agent's accumulated region. Under this contradictory situation for the optimum half-life, it is very important to obtain technologies to control (prolong and shorten) a half-life of the contrast agent.

We used three different types of polymers including PEG-P(Asp(C7F9)x) block copolymers in order to control half-livers in blood. In Table 4, we describe the compositions of the two copolymers other than PEG-P(Asp(C7F9)x). These two copolymers contain hydrophobic poly(L-lactic acid) chains that are expected to work for incorporation of hydrophobic PFC5 into emulsions. Table 5 summarizes five samples prepared from four polymers. By adjusting the vacant volume of a 1.5-mL glass vial to a small value (ca., 300 μL, meaning 1.2 mL of the sample volume.), we successfully obtained emulsions with higher PFC5 contents than 0.4 vol.% in runs 1–3. In these cases, the sonication was carried out at 15 °C. When emulsions were prepared in the same conditions of run 1 except for a different temperature (at 40 °C) and a different vacant volume (ca. 0 μL), the PFC5 content was considerably lower (0.408 vol.%) than in run 1.

Table 4
Compositions of two poly(L-lactic acid)(PLA)-containing polymers.

Code	Structure	Compositions
Gelatin derivative	Poly(L-lactic acid)-grafted gelatin	M.W. of PLA: 1000 weight ratio PLA/gelatin = 0.17
PEG-PLA	Poly(ethylene glycol)-b-Poly(L-lactic acid) Block copolymer	M.W. of PEG: 2000 M.W. of PLA: 1000

We injected these five samples in a mouse tail vein. As shown in Fig. 5, we observed a distinct difference in PFC5 concentrations at 1 min after the injection between three runs containing PLA (runs 1–3) and the other two runs for PEG-P(Asp(C7F9)x). The former three runs showed almost a 100% dose at 1 min with an assumption that blood volume was 7 vol./wt.% of body weight, while the latter two runs provided considerably smaller values than the 100% dose. In all runs, however, PFC5 concentrations were rapidly lowered at 10 and 30 min after the injection, and no clear difference was observed at these time points among all the runs. Therefore, control of pharmacokinetic behaviors, in particular prolongation of blood half-life from a few minutes, was not successfully achieved in this examination by the use of different polymer structures. For the pharmacokinetic control of the emulsions, an additional functional component may be required. Rapoport et al. (Rapoport et al., 2011) reported a very stable circulation (half-life = 2–4 h) in blood for perfluoro-crown-ether compound containing nano-emulsions.

Table 5
Compositions of PFC-emulsions for in vivo experiments.

Run	Polymer	Polymer concentration in feed (%)[a]	PFC5 concentration in feed (vol.%)	PFC5 concentration obtained in emulsion (vol.%)	Cumulant average diameter (nm)
1	Gelatin derivative[b]	1.0	1.25[d]	0.613	345.9
2	Gelatin derivative[b]	4.0	1.25[d]	0.429	542.6
3	PEG-b-PLA[a]	4.0	1.0[d]	0.491	222.6
4	F-15%[c]	4.0	2.0	0.465	256.3
5	F-59%[c]	4.0	1.0	0.670	225.1

[a] Weight (g)/water volume (mL).
[b] Listed in Table 4.
[c] Listed in Table 1.
[d] Sonication at 15 °C.

According to this report, a perfluoro compound showing stable emulsion formation may be utilized for stable incorporation of another PFC.

4. Discussion

In the examinations of this study, we successfully obtained very small (ca. 200 nm in diameter) PFC5-containing emulsions with high PFC5 contents in a very facile method using a common bath-type sonicator. Actually, the used sonicator was the smallest model with the lowest sonication power (max. Input power: 90 W) in its product line. The other facile aspect of this preparation method is the working temperature. By mixing PFC6 we performed the emulsion preparation at 40 °C, which is above the boiling temperature of PFC5. In a conventional method's use of a high-pressure emulsifier, cooling of the whole system is required for evading a large amount evaporation of PFC5 due to heat generated within a high-pressure emulsifier. In contrast, we did not need cooling samples during the preparation. This facileness is substantially important when we consider a scale-up of the emulsion preparations. In a large-scale production of these emulsions, the heat generated in preparation processes (both in emulsification and sonication) may become large enough to raise a temperature of the solution above the boiling temperature. Therefore, successful preparations at a high temperature means that there is a large margin for large-scale preparation with high PFC5 content as well as easy handling of samples at room temperature throughout the sonication procedure.

We could not substantially change pharmacokinetic behaviors of the PFC5-containing emulsion, even when using different polymers. This is a very different situation from polymeric micelle drug carrier cases where block polymer structure was revealed to be a very influential factor on pharmacokinetic behaviors of the incorporated drug into the polymeric micelles (Yokoyama, 2005, 2007; Watanabe et al., 2006). This difference may result from the liquid state of the emulsion's core, while the solid core is essential for stable drug incorporation in the polymeric micelle systems. An alternative and novel method may be required to obtain stable incorporation of liquid PFC for dramatically changed pharmacokinetics.

5. Conclusion

By using a bath-type sonicator, we successfully obtained PFC5-containing emulsions in a diameter range of 200 nm. These emulsions are very potent for theranostics of solid tumors through ultrasound irradiation. Furthermore, these emulsions were prepared in high PFC5 yields at 40 °C, which is higher than the boiling temperature of PFC5. This very facile preparation method is an important technological key for large-scale production of these medically valuable emulsions.

Acknowledgements

This work was supported by the New Energy and Industrial Technology Development Organization, Japan. M. Yokoyama, K. Shiraishi, and M. Nishihara acknowledge support from the JST CREST program, Grant-in-Aid of the Ministry of Education, Culture, Sports, Science and Technology, Japan, and Kanagawa Academy of Science and Technology. The authors acknowledge Dr. Kenichi Kawabata and Dr. Rei Asami of Central Research Laboratory, Hitachi, Ltd., for their valuable discussion on PFC-containing nanoemulsions.

Appendix A. Supplementary data

Supplementary data associated with this article can be found, in the online version, at doi:10.1016/j.ijpharm.2011.10.006.

References

Ai, H., 2011. Layer-by-layer capsules for magnetic resonance imaging and drug delivery. Adv. Drug Deliv. Rev. 63, 772–788.
Asami, R., Azuma, T., Kawabata, K., 2009. Fluorocarbon droplets as next generation contrast agents—their behavior under 1–3 mhz ultrasound. IEEE Proc. Int. Ultrasonics Symp., 1294–1297.
Asami, R., Ikeda, T., Azuma, T., Kawabata, K., Umemura, S., 2010. Acoustic signal characterization of phase change nanodroplets in tissue-mimicking phantom gels. Jpn. J. Appl. Phys. 49, 07HF16.
Blanco, E., Kessinger, C.W., Sumer, B.D., Gao, J., 2009. Multifunctional micellar nanomedicine for cancer therapy. Exp. Biol. Med. 234, 123–131.
Bryson, J.M., Fichter, K.M., Chu, W.J., Lee, J.H., Li, J., Madsen, L.A., McLendon, P.M., Reineke, T.M., 2009. Polymer beacons for luminescence and magnetic resonance imaging of DNA delivery. Proc. Natl. Acad. Sci. U.S.A. 106, 16913–16918.
Chen, X.S., 2011. Introducing theranostics journal—from the editor-in-chief. Theranostics 1, 1–2.
Gianella, A., Jarzyna, P.A., Mani, V., Ramachandran, S., Calcagno, C., Tang, J., Kann, B., Dijk, W.J., Thijssen, V.L., Griffioen, A.W., Storm, G., Fayad, Z.A., Mulder, W.J., 2011. A multifunctional nanoemulsion platform for imaging guided therapy evaluated in experimental cancer. ACS Nano 5, 4422–4433.
Grishenkov, D., Pecorari, C., Brismar, T.B., Paradossi, G., 2009. Characterization of acoustic properties of PVA-shelled ultrasound contrast agents: ultrasound-induced fracture (part II). Ultrasound Med. Biol. 35, 1139–1147.
Hernot, S., Klibanov, A.L., 2008. Microbubbles in ultrasound-triggered drug and gene delivery. Adv. Drug Deliv. Rev. 60, 1153–1166.
Ishida, O., Maruyama, K., Sasaki, K., Iwatsuru, M., 1999. Size-dependent extravasation and interstitial localization of polyethyleneglycol liposomes in solid tumor-bearing mice. Int. J. Pharm. 190, 49–56.
Jeong, H., Huh, M., Lee, S.J., Koo, H., Kwon, I.C., Jeong, S.Y., Kim, K., 2011. Photosensitizer-conjugated human serum albumin nanoparticles for effective photodynamic therapy. Theranostics 1, 230–239.
Kaida, S., Cabral, H., Kumagai, M., Kishimura, A., Terada, Y., Sekino, M., Aoki, I., Nishiyama, N., Tani, T., Kataoka, K., 2010. Visible drug delivery by supramolecular nanocarriers directing to single-platformed diagnosis and therapy of pancreatic tumor model. Cancer Res. 70, 7031–7041.
Kalber, T.L., Kamaly, N., Higham, S.A., Pugh, J.A., Bunch, J., McLeod, C.W., Miller, A.D., Bell, J.D., 2011. Synthesis and characterization of a theranostic vascular disrupting agent for in vivo MR imaging. Bioconjug. Chem. 22, 879–886.
Kamaly, N., Miller, A.D., 2010. Paramagnetic liposome nanoparticles for cellular and tumour imaging. Int. J. Mol. Sci. 11, 1759–1776.
Kawabata, K., Sugita, N., Yoshikawa, H., Azuma, T., Umemura, S., 2005. Nanoparticles with multiple perfluorocarbons for controllable ultrasonically induced phase shifting. Jpn. J. Appl. Phys. 44, 4548–4552.
Kawabata, K., Asami, R., Yoshikawa, H., Azuma, T., Umemura, S., 2010a. Acoustic response of microbubbles derived from phase-change nanodroplet. Jpn. J. Appl. Phys. 49, 07HF18.
Kawabata, K., Asami, R., Yoshikawa, H., Azuma, T., Umemura, S., 2010b. Sustaining microbubbles derived from phase change nanodroplet by low-amplitude ultrasound exposure. Jpn. J. Appl. Phys. 49, 07HF20.
Kim, K., Kim, J.H., Park, H., Kim, Y.S., Park, K., Nam, H., Lee, S., Park, J.H., Park, R.W., Kim, I.S., Choi, K., Kim, S.Y., Park, K., Kwon, I.C., 2010. Tumor-homing multifunctional nanoparticles for cancer theragnosis: simultaneous diagnosis, drug delivery, and therapeutic monitoring. J. Contr. Rel. 146, 219–227.
Lammers, T., Kiessling, F., Hennink, W.E., Storm, G., 2010. Nanotheranostics and image-guided drug delivery: current concepts and future directions. Mol. Pharm. 7, 1899–1912.
Lammers, T., Aime, S., Hennink, W.E., Storm, G., Kiessling, F., 2011. Theranostic Nanomedicines. Acc. Chem. Res. 44, 1029–1038.
Litzinger, D.C., Buiting, A.M.J., van Rooijen, N., Huang, L., 1994. Effect of liposome size on the circulation time and intraorgan distribution of amphipathic poly(ethylene glycol)-containing liposomes. Biochim. Biophys. Acta 1190, 99–107.
MacKay, J.A., Li, Z., 2010. Theranostic agents that co-deliver therapeutic and imaging agents? Adv. Drug Deliv. Rev. 62, 1003–1004.
Min, K.H., Kim, J.H., Bae, S.M., Shin, H., Kim, M.S., Park, S., Lee, H., Park, R.W., Kim, I.S., Kim, K., Kwon, I.C., Jeong, S.Y., Lee, D.S., 2010. Tumoral acidic pH-responsive MPEG-poly(beta-amino ester) polymeric micelles for cancer targeting therapy. J. Contr. Rel. 144, 259–266.
Mohan, P., Rapoport, N., 2010. Doxorubicin as a molecular nanotheranostic agent: effect of doxorubicin encapsulation in micelles or nanoemulsions on the ultrasound-mediated intracellular delivery and nuclear trafficking. Mol. Pharm. 6, 1959–1973.
Moon, G.D., Choi, S.W., Cai, X., Li, W., Cho, E.C., Jeong, U., Wang, L.V., Xia, Y., 2011. A new theranostic system based on gold nanocages and phase-change materials with unique features for photoacoustic imaging and controlled release. J. Am. Chem. Soc. 133, 4762–4765.
Nagayasu, A., Uchiyama, K., Nishida, T., Yamagiwa, Y., Kawai, Y., Kiwada, H., 1996. Is control of distribution of liposomes between tumors and bone marrow possible? Biochim. Biophys. Acta 1278, 29–34.
Nakamura, E., Makino, K., Okano, T., Yamamoto, T., Yokoyama, M., 2006. A polymeric micelle MRI contrast agent with changeable relaxivity. J. Contr. Rel. 114, 325–333.
Nishihara, M., Imai, K., Yokoyama, M., 2009. Preparation of perfluorocarbon/fluoroalkyl polymer nanodroplets for cancer-targeted ultrasound contrast agents. Chem. Lett. 38, 556–557.